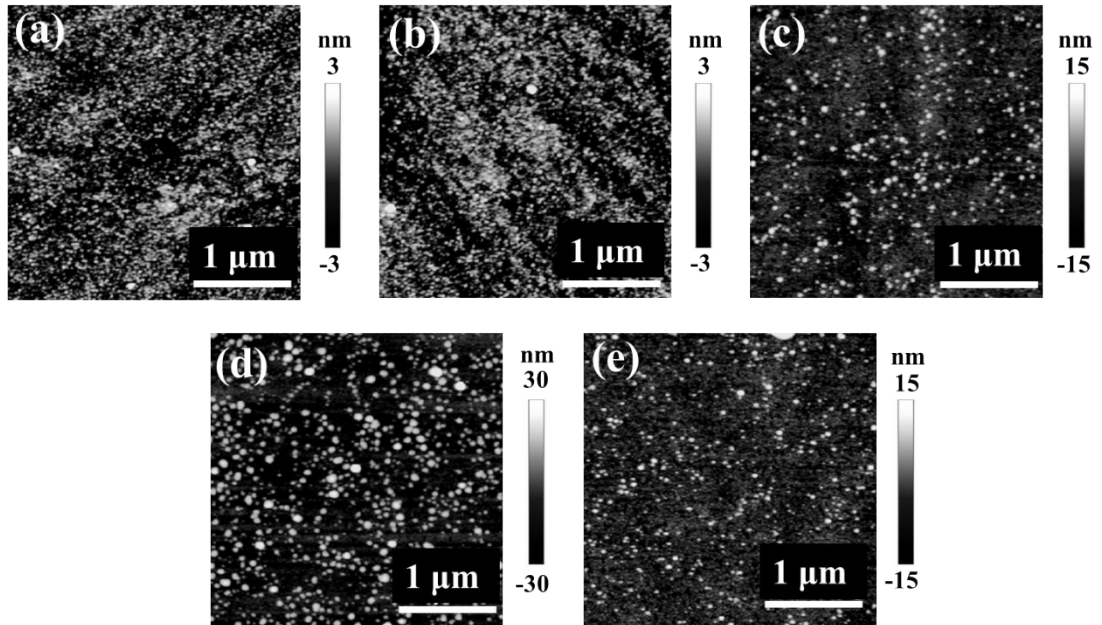
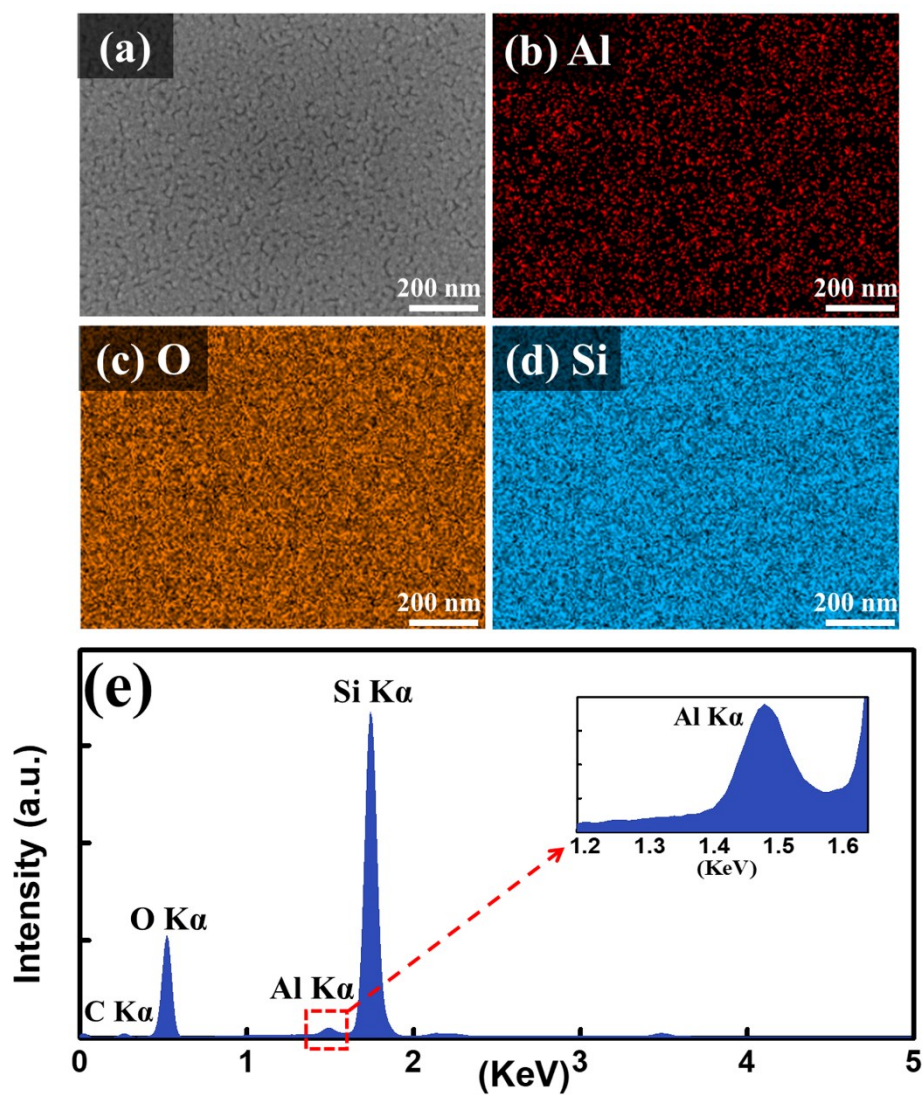


**Fig. S1** Annealing temperature effect on the fabrication of the self-assembled stalagmite-shaped Al nanoparticles (NPs) with an identical deposition thickness of 6 nm. (a) - (e) Atomic force microscope (AFM) top views of the samples with a size of  $1 \times 1 \mu\text{m}^2$ . (a-1) - (e-1) The cross-sectional line-profiles obtained from the blue lines drawn in AFM top-views. (a-2) - (e-2) 2D fast Fourier transform (FFT) spectra of the samples.



**Fig. S2** Evolution of the self-assembled stalagmite-shaped Al nanoparticles NPs fabricated at various temperatures with the deposition thickness of 6nm. (a) - (e) AFM top-views of  $3 \times 3 \mu\text{m}^2$ .



**Fig. S3** (a) SEM image of the packed Al NPs that fabricated at 200°C with the deposition thickness of 6nm. (b) – (d) the element distribution map of (b) Al (Red), (c) O (Blue) and (d) Si (Orange) acquired from the location shown in the SEM image respectively.(e) The corresponding energy dispersive X-ray spectroscopy (EDS) spectrum.

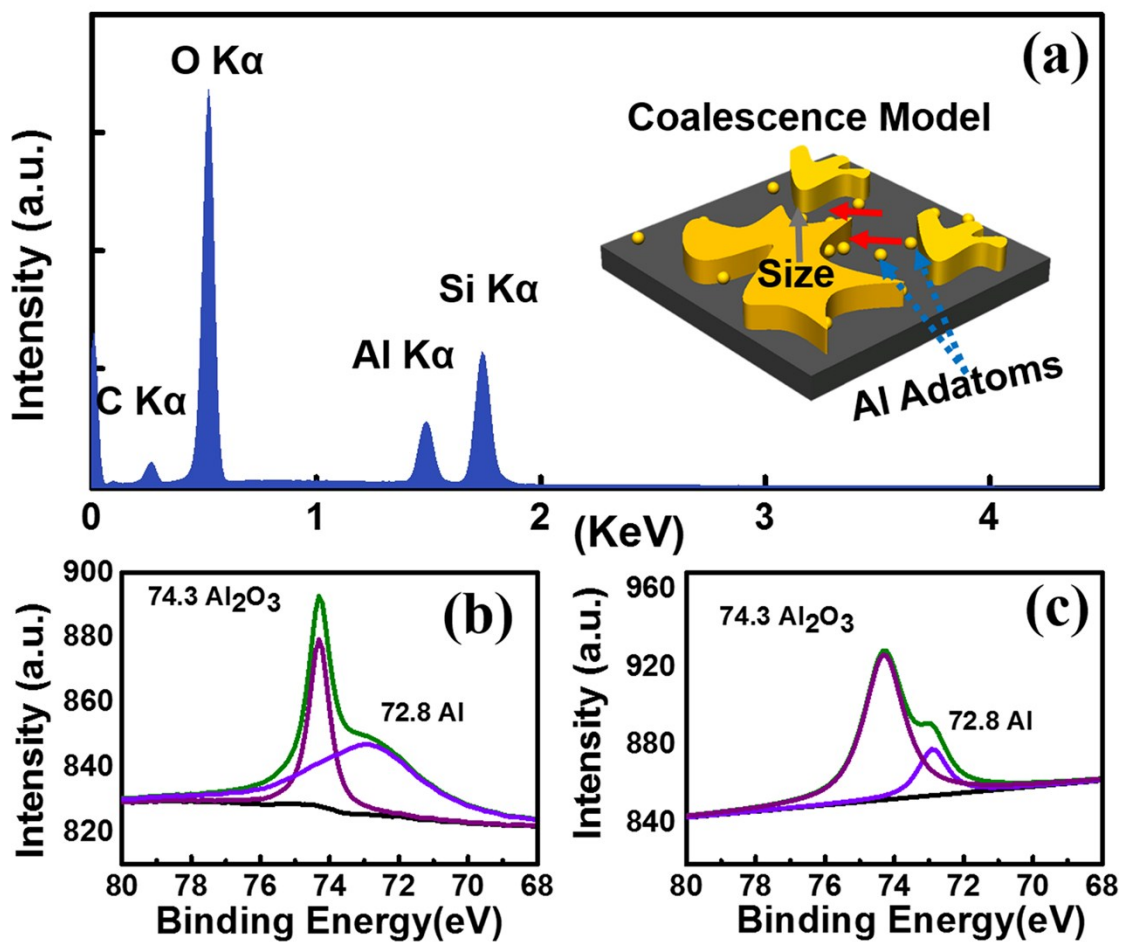


**Fig. S4** (a) Energy dispersive X-ray spectroscopy (EDS) spectra acquired from the Al nanostructures (NSs) fabricated with 20 nm deposition thicknesses.(b) X-ray photoelectron spectroscopy spectra obtained from the as-deposited substrate with 6 nm Al and (c) Al NPs fabricated at 650 °C

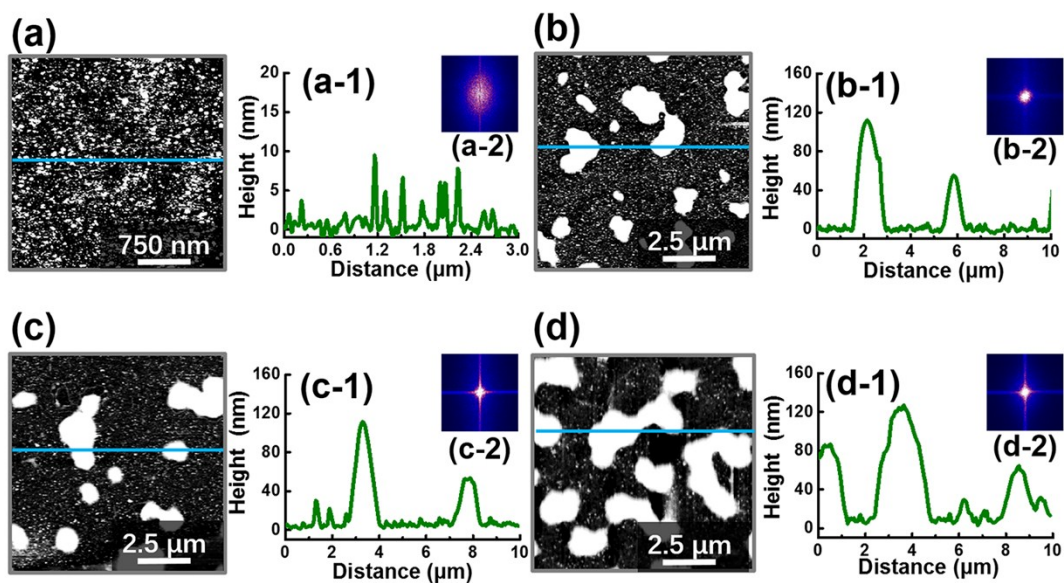


**Fig. S5** Self-assembled Al NSs fabricated at annealing temperatures 650 °C for 900 s. (a) - (e) AFM top views ( $10 \times 10 \mu\text{m}^2$ ) of the samples with various deposition thicknesses between 6 and 20 nm. The corresponding (a-1) - (e-1) cross-sectional line-profiles and (a-2) - (e-2) 2D FFT spectra of the samples.

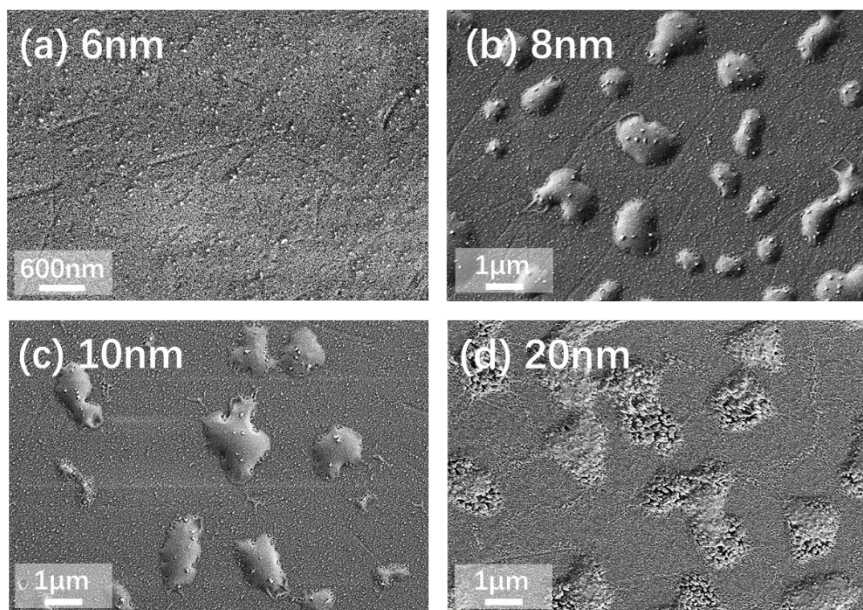


**Fig. S6** SEM images of the self-assembled Al NSs fabricated at 650°C for 900s. (a) - (d) The deposition thicknesses varied from 6 to 20 nm.

### Calculation of enhancement factors (EF)

We calculated the EF induced by surface enhanced Raman scattering with

the formula  $EF = \frac{I_{SERS}}{I_0} \times \frac{N_0}{N_{SERS}}$ , where  $I_{SERS}$  and  $I_0$  are the peak intensities of the Raman signals obtained from the SERS substrates and bare quartz substrate, respectively.  $N_0$  is the total amount of adenine molecules in laser spot, and  $N_{SERS}$  is the absorbed molecules in hot spot regions.  $N_0/N_{SERS}$  was calculated by the following

equation:  $\frac{N_0}{N_{SERS}} = \frac{N_A \times V \times c \times \frac{S_L}{S_A}}{S_L \times \rho \times N_{HS}}$ , where  $N_A$  is the Avogadro constant,  $V$  is the droplet volume of adenine solution, (20  $\mu$ L), and  $c$  is the adenine concentration of 1 mM.  $S_L$  is the spot area under laser illumination,  $S_A$  is the area of dried adenine droplet (with a diameter of  $\sim 0.5$  cm), and  $\rho$  indicates the average density of the Al NPs.  $N_{HS}$ , the contributed adenine molecules within the hot spot regions between two NPs, can be

calculated with  $N_{HS} = \frac{V_{HS}}{V_m}$ . Here,  $V_m$  is the volume of the adenine molecule (with a diameter of  $\sim 2$  nm), and  $V_{HS}$  denotes the average volume of the hot spot region ( $|E/E_0|^4 > 1/2|E_{max}/E_0|^4$ ), which estimated by the FDTD simulation. The area ratio ( $\gamma$ ) of the Al

NSs can be defined by  $\gamma = \frac{S_{NS}}{S_{Total}}$ , where  $S_{NS}$  is the area that occupied by Al, and  $S_{Total}$  is the total area throughout the characterized region from AFM top-views. Thus, for the worm-like Al nano-mounds (NMs), the EF can be evaluated from the stalagmite-shaped

Al NPs, namely,  $EF_{NMs} = \frac{\gamma_{NM}}{\gamma_{NP}} \times EF_{NP}$ .

### **FDTD simulation**

Commercial software FDTD solution (Lumerical) was employed to simulate the EM distribution of the resultant Al NSs. The size of the Al NSs was derived from the statistical results according to the AFM top-views. To simulate the EM field distribution, a 325 nm plane-wave with the polarized E-field direction parallel to the z-axis were engaged as excited source along z-axis. The boundary condition in z-axis and x-axis direction were established with periodical condition, and the perfectly matched layer condition was applied for y-axis. To get relatively high resolution, the mesh grid size was set as 0.5 nm in x-y-z direction, and shutoff level was  $10^{-6}$ , respectively.

**Table 1** Summary of the average height (AH), density, average diameter (AD), distance, root-mean-squared roughness ( $R_{RMS}$ ), and surface area difference (SAD) of the samples fabricated at various annealing temperatures from 200 to 650 °C for 900 s.

<b>AT (°C)</b>	<b>AH (nm)</b>	<b>Density (<math>10^{10}/\text{cm}^2</math>)</b>	<b>AD (nm)</b>	<b>Distance (nm)</b>	<b><math>R_{RMS}</math> (nm)</b>	<b>SAD (%)</b>
0	2.3	6.45	25.0	28.3	0.8	0.4
200	2.7	6.22	28.0	30.7	0.8	0.4
500	8.1	0.87	45.2	93.8	2.5	3.0
600	19.9	0.78	63.1	99.1	5.2	7.0
650	11.5	0.75	42.2	92.2	2.2	2.2

**Table 2** The peak intensity ( $I_{\text{SERS}}$ ) and enhancement factor (EF) of the Raman vibrational modes at 1248, 1332, 1484, and 1601  $\text{cm}^{-1}$  from the sample fabricated at various temperatures.

	Peak Position ( $\text{cm}^{-1}$ )	Annealing Temperature ( $^{\circ}\text{C}$ )				
		0	200	500	600	650
$I_{\text{SERS}}$	1248	32	28	27	20	12
	1332	91	82	77	57	33
	1484	45	40	37	28	17
	1601	21	19	18	13	8
EF ( $\times 10^7$ )	1248	3.22	2.94	0.99	0.37	0.52
	1332	3.49	3.26	1.10	0.43	0.55
	1484	2.52	2.34	7.66	0.30	0.41
	1601	2.85	2.73	9.30	0.34	0.45

**Table 3** The  $I_{\text{SERS}}$  and EF of the Raman peaks at 1248, 1332, 1484, and 1601  $\text{cm}^{-1}$  from adenine molecules on substrates fabricated at various deposition thicknesses between 8 and 20 nm.

	Peak Position ( $\text{cm}^{-1}$ )	Deposition Thickness (nm)		
		8	10	20
$I_{\text{SERS}}$	1248	6	13	16
	1332	22	41	51
	1484	10	20	24
	1601	5	9	12
$\text{EF}$ ( $\times 10^6$ )	1248	0.25	0.55	0.47
	1332	0.33	0.64	0.58
	1484	0.23	0.47	0.40
	1601	0.27	0.51	0.47